Available online at www.sciencedirect.com

SCIENCE DIRECT

European Journal of Pharmacology 513 (2005) 21–33

www.elsevier.com/locate/ejphar

Gene expression of energy and protein metabolism in hearts of hypertensive nitric oxide- or GSH-depleted mice

Helena Chon[a], Hans A.R. Bluyssen[a], Frank C.P. Holstege[b], Hein A. Koomans[a], Jaap A. Joles[a], Branko Braam[a,*]

[a]*Department of Nephrology and Hypertension, University Medical Center, F03.223, PO Box 85500, 3508 GA Utrecht, Netherlands*
[b]*Genomics Laboratory, University Medical Center Utrecht, Utrecht, Netherlands*

Received 7 October 2004; received in revised form 25 January 2005; accepted 31 January 2005
Available online 22 April 2005

Abstract

Hypertension demands cardiac synthetic and metabolic adaptations to increased afterload. We studied gene expression in two models of mild hypertension without overt left ventricular hypertrophy using the NO synthase inhibitor nitro-L-arginine (L-NNA) and the glutathione depletor buthionine-*S*,*R*-sulfoximine (BSO). Mice were administered L-NNA, BSO, or water for 8 weeks. RNA of left ventricles was pooled per group, reverse transcribed, Cy3 and Cy5 labeled, and hybridized to cDNA microarrays. Normalized $\log_2$ Cy3/Cy5 ratios of ≥ 0.7 or ≤ -0.7 were considered significant. L-NNA and BSO both caused hypertension. Gene expression was regulated in cytoskeletal components in both models, protein synthesis in L-NNA-treated mice, and energy metabolism in BSO-treated mice. Energy metabolism genes shared several common transcription factor-binding sites such as Coup-Tf2, of which gene expression was increased in BSO-treated mice, and COMP-1. Characterization of the left ventricular adaptations as assessed with gene expression profiles reveals differential expression in energy and protein metabolism related to the pathogenetic background of the hypertension.

Keywords: Oxidative stress; Hypertension; Gene expression; Left ventricular hypertrophy; Energy metabolism

1. Introduction

Hypertension is associated with increased workload to the heart. This eventually leads to cardiac hypertrophy. Before these structural alterations take place, a heart that is exposed to high pressure mobilizes compensatory mechanisms, such as improvement of contractile force (Bartunek et al., 2000). Metabolic adaptations consist of decreased fatty acid metabolism as well as increased anaerobic glycolysis in order to maintain ATP production for contractile force in a state where oxygen supply is insufficient (Depre et al., 1998; Sambandam et al., 2002). Further adaptation to pressure overload is achieved by expansion of myocytes resulting in left ventricular hypertrophy. Protein synthesis is enhanced in pressure overload models and is an indicator of left ventricular hypertrophy (Lim et al., 2001; Nagatomo et al., 1999; Wada et al., 1996).

Most, if not all, cardiovascular risk factors lead to a disturbance of the balance between nitric oxide (NO) and superoxide ($O_2^{\bullet -}$). Models are available for NO depletion and for $O_2^{\bullet -}$ excess. NO depletion can readily be achieved by inhibition of nitric oxide synthase (NOS) with nitro-L-arginine (L-NNA) and is associated with hypertension and with cardiac complications in some (Verhagen et al., 2000; Zhang et al., 2003), but not all (Bartunek et al., 2000; Matsubara et al., 1998) experimental models. Glutathione depletion by inhibition of gamma-glutamylcysteine synthetase using buthionine-*S*,*R*-sulfoximine (BSO) leads to hypertension when administered chronically (Vaziri et al., 2000). The diminished antioxidant capacity due to glutathione depletion leads to excess of $O_2^{\bullet -}$. As such, NOS

* Corresponding author. Tel.: +31 30 2507329; fax: +31 30 2543492.
E-mail address: G.B.Braam@azu.nl (B. Braam).

0014-2999/$ - see front matter © 2005 Elsevier B.V. All rights reserved.
doi:10.1016/j.ejphar.2005.01.054

inhibition and glutathione depletion will affect NO/$O_2^{\bullet-}$ balance but through entirely different mechanisms.

We investigated which cardiac gene expression changes occur in the left ventricle of mice subjected to either decreased NO or to increased $O_2^{\bullet-}$ availability without apparent left ventricular hypertrophy. Direct comparison of two different hypertension models may allow for analysis of pressure-dependent, pharmacology-independent effects on the cardiac adaptations. We hypothesized that NO depletion and $O_2^{\bullet-}$ excess affect left ventricular gene expression in distinct ways, in particular with respect to energy metabolism and left ventricular hypertrophy. Specific questions were (1) how gene expression is affected in hearts of hypertensive mice with NO depletion or $O_2^{\bullet-}$ excess; (2) if patterns of gene expression can be discerned that are related to increased work load resulting in adapted contractility and metabolism, hypertrophy or altered redox balance; and (3) if clusters of genes could be related to common transcription factors.

2. Materials and methods

2.1. Animals

Female C57Bl/6J mice weighing 20–25 g (Harlan-Olac, Blackthorn, UK) were exposed to a 12 h light/dark cycle, an ambient temperature of 22 °C and a humidity of 60%. Sentinel animals, which were monitored regularly for infection, consistently tested negatively for infection by nematodes and pathogenic bacteria, and for antibodies to a large number of rodent viral pathogens (International Council for Laboratory Science Nijmegen, Netherlands) throughout the experiment. The Utrecht University Board for studies in experimental animals approved the studies.

2.2. Treatment

Three groups of mice were studied. L-NNA (0.5 g/l, Sigma Chemical Co., St Louis, MO, $n=13$) or BSO (3 g/l, Sigma, $n=13$) was administered in demineralized water ad libitum for eight weeks. Control mice ($n=12$) received no treatment. For RNA analyses, animals were either used for the microarray experiments or for Reverse Transcription-Polymerase Chain Reaction (RT-PCR) confirmation. Water intake and body weight were measured regularly.

2.3. Blood pressure measurements

Systolic blood pressure of preheated mice was measured every 2 weeks in a fan-controlled chamber at 37 °C for 10 min using a tail-cuff (IITC, San Diego, CA), starting 1 week before treatment. In each session, at least two measurements per animal were averaged. Two training sessions preceded all actual measurements.

2.4. Urine collection

Overnight urine was collected every two weeks by placing the animals in metabolic cages for 18 h (16:00–10:00). During this period, mice were restricted from food to prevent confounding nitrate excretion resulting from dietary intake. Instead, they had access to drinking water with 2% glucose as an alternative energy source and to increase water intake and urine production. Urine was chilled immediately after collection and stored at 4 °C for protein and creatinine determination or at −80 °C for biochemical measurements.

2.5. Tissue isolation

After 8 weeks, mice were anesthetized with an i.p. injection of ketamine (46.7 mg/ml), xylazine (8 mg/ml), and atropine (0.067 mg/ml). Blood was collected in pre-chilled EDTA tubes through puncture of the retro-orbital plexus. The heart and liver were isolated, blotted dry, immediately weighed, dissected further while on ice, and frozen in liquid nitrogen. Samples were stored at −80 °C until further analysis.

2.6. Biochemical measurements

Urinary creatinine levels were determined colorimetrically (Sigma). Urinary protein concentration was determined by the Bradford method (Bradford, 1976). Urinary excretion of stable metabolites of NO; NO_2 and NO_3 (NOx) was measured by the formation of L-^{3}H-citrulline from L-^{3}H-arginine using the Cayman NOx assay kit (Attia et al., 2002). Urinary lipid peroxides were determined by measurement of thiobarbituric acid reactive substances (Attia et al., 2003). In short, aliquots of 500 μl of urine were mixed with 500 μl of 1% thiobarbituric acid (pH 1.5), boiled for 30 min, and then cooled down to room temperature. The absorbance was measured at 540 nm using a microplate reader. All urinary results were corrected using creatinine excretion. Hepatic GSH was measured with the Cayman's GSH assay kit. The reaction between GSH and 5,5′-dithiobis-2-nitrobenzoic acid was catalyzed using GSH reductase, yielding the product 5-thio-2-nitrobenzoic acid, which was colored with Ellman's reagent. GSSG was first converted into GSH by adding NADPH. GSSG alone was measured by removing GSH first with *N*-ethylmaleimide. Subtraction of total GSH with GSSG resulted in GSH values.

2.7. RNA isolation

Tissue was homogenized in a MiniBeadBeater (Biospec Products Inc., Bartlesville, OK) in Trizol solution (Invitrogen Life Sciences, Carlsbad, CA) using glass beads (∅ 1 mm) for 30 s. RNA was extracted from homogenates using the TRIzol procedure (Invitrogen) and quantified as described before (Hoenderop et al., 2004).

2.8. Reverse transcription/labeling

Samples that were designated for microarray experiments were pooled per group ($n=8$ for L-NNA or BSO; $n=4$ for control) in equal amounts of total RNA per subject. Reverse transcription was performed as described before (Hoenderop et al., 2004). The control sample was labeled with Cy3, and the L-NNA and BSO samples were labeled with Cy5.

2.9. Hybridization and scanning/quantification

Mouse NIH 15K cDNA microarrays (Ontario Microarray Centre, Toronto University, Canada) were used. Hybridization experiments and scanning were carried out as described before (Hoenderop et al., 2004). Genes were considered significantly regulated when $\log_2$ transformed ratios were ≥ 0.7 (1.6 fold change) or ≤ -0.7.

2.10. Clustering analysis and gene ontology annotations

Hierarchical clustering of microarray data was performed using the Expression Profiler tool EPCLUST (Jaak Vilo, EBI). Average linkage clustering based on correlation measure-based distance was performed on data for which ratios were ≥ 0.7 or ≤ -0.7 in at least one of two situations. Ratios of the genes were coupled to the Biological Processes classification of the Gene Ontology (GO) Consortium (Ashburner et al., 2000) using proprietary software and Access 2000 (Microsoft Corporation, Redmond, WA). For each Biological Process category, the total number of annotated genes and the percentage of significantly regulated genes was counted, and the average ratio was calculated. Interesting categories were defined as groups containing at least 10 genes and at least 15% of genes significantly up or downregulated.

2.10.1. Analysis of transcription factor binding sites

Using Genomatix MatInspector Professional (Release 7.0 Sept. 2003) (Werner, 2001) putative transcription factor binding sites were searched in the cluster of glycolytic and respiratory chain genes that were regulated in BSO-treated mice. To minimize the chance of false positive calls, a negative control set of genes with ratios between 0.01 and −0.01 for L-NNA and BSO was tested using the same settings (in total 19 genes). Only transcription factor binding sites up to 1000 base pairs upstream of the coding region with a similarity matrix score higher than the optimized matrix similarity and a transcription factor binding site frequency that exceeded the frequency of the negative control set by 0.4 were considered.

2.11. RT-PCR confirmation

RNA samples of mice designated for RT-PCR confirmation ($n=2$–3) were individually processed. RT-PCR experiments were performed as described before (Chon et al., 2004). Results were quantified as 18S-corrected mean intensities. The primers and conditions used for PCR are summarized in the Supplementary Table 1.

2.12. Statistics of systolic blood pressure and biochemical measurements

Data are presented as mean ± S.E.M. Measurements were compared with one-way ANOVA or, where appropriate, two-way ANOVA for repeated measures, followed by Student–Newman–Keuls test. $P<0.05$ was considered significant.

3. Results

3.1. L-NNA and BSO caused hypertension but no proteinuria or left ventricular hypettrophy

After 2 weeks of treatment, systolic blood pressure was 92 ± 2 mmHg in controls and significantly higher ($P<0.01$ vs. control) in L-NNA- and BSO-treated animals (107 ± 2 mmHg and 100 ± 2 mmHg, respectively, Fig. 1A). After 8 weeks of treatment, systolic blood pressure further increased

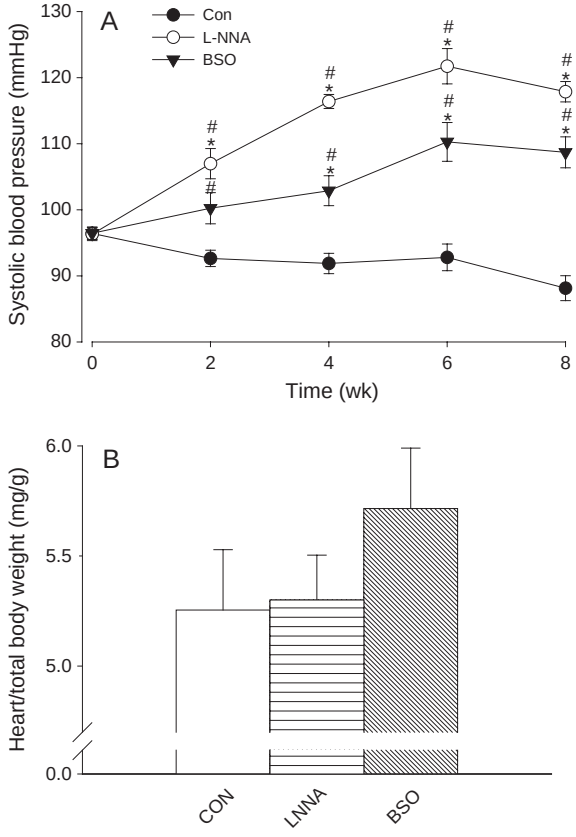

Fig. 1. Tail-cuff systolic blood pressure measurements followed during the experiment (A) and heart weights corrected for total body weight at 8 weeks (B) in mice treated with L-NNA or BSO and controls. *$P<0.001$ compared to con at same time; #$P<0.001$ compared to $t=0$ of same group.

to 118 ± 2 mmHg in L-NNA-treated mice ($P < 0.001$ vs. control) and to 109 ± 2 mmHg in BSO-treated animals ($P < 0.001$ vs. control). Untreated mice maintained normal systolic blood pressure (88 ± 2 mmHg). Body weights were lower in BSO-treated mice (21.0 ± 0.4 g) compared to control (22.8 ± 0.4 g, $P < 0.05$), but were not different from L-NNA-treated mice (22.0 ± 0.4 g). The treatments did not result in proteinuria (0.35 ± 0.04, 0.24 ± 0.02 and 0.33 ± 0.04 mg/mg creatinine for L-NNA, BSO and controls, respectively). Total heart/body weights at 8 weeks showed no difference between the groups (5.3 ± 0.2 mg/g with L-NNA, 5.7 ± 0.3 mg/g with BSO and 5.3 ± 0.3 mg/g in controls; Fig. 1B).

3.2. NOx, thiobarbituric acid reactive substances, and tissue GSH content in L-NNA and BSO treated mice

Urinary excretion of NOx and thiobarbituric acid reactive substances were regarded as indicators of whole body production of NO and reactive oxygen species, respectively. Baseline urinary NOx excretion was not different between groups, however, after 8 weeks of treatment, NOx excretion was decreased in both L-NNA (0.142 ± 0.030 μmol/mg creatinine, $P < 0.001$) and BSO-treated animals (0.302 ± 0.052 μmol/mg creatinine, $P < 0.01$) as compared to controls (0.569 ± 0.070 μmol/mg creatinine) (Fig. 2A). Urinary NOx excretion was also lower in the L-NNA-treated animals as compared to BSO-treated animals ($P < 0.05$). Urinary thiobarbituric acid reactive substances excretion was increased in BSO-treated mice (5.81 ± 0.94 μmol/mg creatinine) compared to controls (2.92 ± 0.86 μmol/mg creatinine, $P < 0.05$), but not in L-NNA-treated mice (3.41 ± 0.68 μmol/mg creatinine; NS; Fig. 2B). Total GSH was lower in BSO-treated mice than in controls (2.7 ± 0.4 and 5.2 ± 0.2 nmol/mg liver, respectively, $P < 0.05$; Fig. 2C). GSH in L-NNA-treated mice was not affected (5.8 ± 0.2 nmol/mg liver; Fig. 2C). Liver/body weight ratios were not different between groups (45.1 ± 1.2, 45.6 ± 1.0 and 45.7 ± 1.3 mg/g for controls, L-NNA and BSO, respectively).

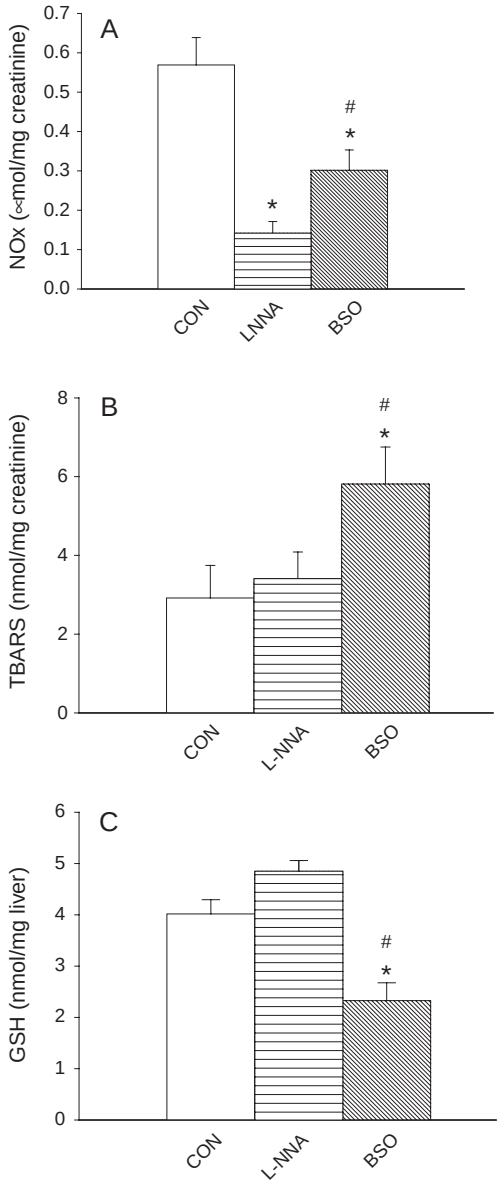

Fig. 2. Oxidative stress parameters urinary NOx excretion (A), thiobarbituric acid reactive substances excretion (B) and liver total glutathione content corrected for total liver weight (C) in mice treated with L-NNA or BSO and controls at 8 weeks. *$P < 0.05$ compared to controls; #$P < 0.05$ compared to L-NNA.

3.3. L-NNA and BSO treatment resulted in differential gene expression in the left ventricle

Chronic treatment with BSO and L-NNA resulted in altered gene expression in left ventricles (3.7% and 7.1% of all 15600 cDNA clones, respectively). The ratio distribution of the two comparisons is shown in Fig. 3A. Note that for the L-NNA comparison the distribution is wider than that for the BSO comparison, indicating that more changes were induced by L-NNA treatment. Genes that are most pronouncedly differentially expressed are displayed in Table 1A–D.

Ribosomal protein Rplp1 and Rpl8, two 60S acidic ribosomal proteins involved in the elongation step in protein synthesis, were upregulated with both L-NNA and BSO (Table 1A and B). Moreover, Rps18 was upregulated in the L-NNA group. Gelsolin is a calcium-dependent actin filament-severing protein that regulates cardiac L-type calcium channels (Lader et al., 1999) and is upregulated in human failing hearts (Yang et al., 2000), was upregulated in both models. Ferritin light chain, has been reported to be downregulated at the transcriptional level in coronary arteries in patients with coronary artery disease (You et al., 2003), however, was strongly upregulated in both conditions in the current experiment (with two representations in the top-10 list of BSO, Table 1B). Moreover, ferritin heavy chain was also upregulated in BSO-treated mice (not shown in Table 1). Polyubiquitin is

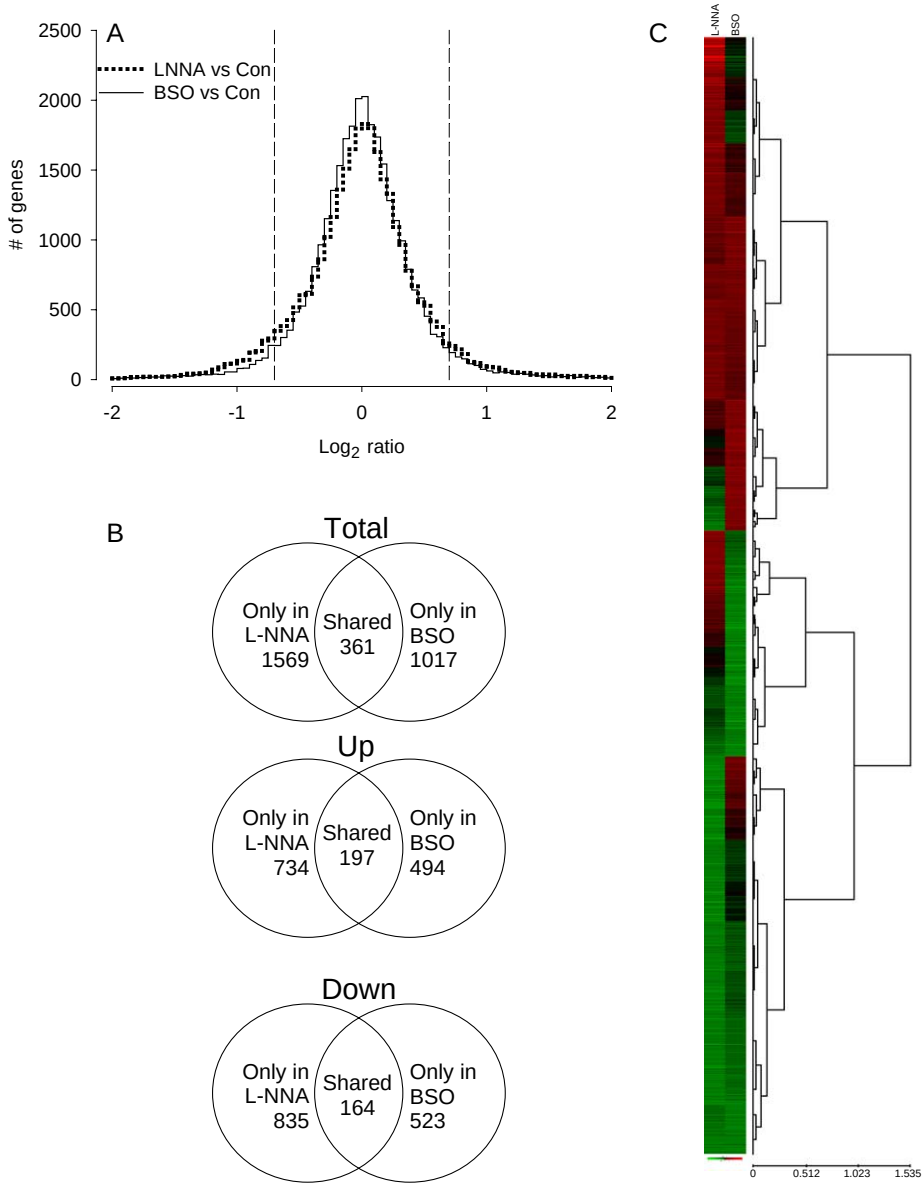

Fig. 3. Global gene expression analysis. Distribution of ratios of all genes are displayed in bins of 0.05 (A). Venn diagrams show co-regulation of genes (B), shown for all genes (top) upregulated (middle), and downregulated genes (bottom). Hierarchical clustering analysis diagram (C) shows global regulation of genes for mice treated with L-NNA (left) and BSO (right).

strongly upregulated by L-NNA and BSO within the top-10 for both (Table 1A and B).

3.4. Analysis of co-regulation of genes

Although the two models act via different mechanisms, a considerable number of differentially expressed genes were regulated in the left ventricles of both BSO- and L-NNA-treated mice (Fig. 3A–C). Hierarchical cluster analysis underscores the similarities in gene expression profiles from L-NNA and BSO-treated animals. Co-regulated genes are summarized in Supplementary Table 2. Among the genes that were not previously mentioned in Table 1, some other interesting genes could be grouped into functional groups. First, metabolism genes, such as glyceraldehyde-3-phosphate dehydrogenase (Gapdh), glucose phosphate isomerase 1 (Gpi1), hydroxylacyl-coenzyme A dehydrogenase (Hadh), enoyl coenzyme A hydratase 1 (Ech1), and cytochrome oxidase subunit Cox4 (two representations) were all induced. Second, two ribosomal proteins, i.e. Rps14 and Rps15, as well as the translation elongation factor 1-beta (Eef1b) were upregulated. Finally, two cytoskeleton-related genes, tropomyosin isoform 2 and tubulin cofactor A, were upregulated.

3.5. Analysis of functional groups using GO Consortium classifications of biological processes

All genes were coupled to the Biological Processes classification of the GO Consortium. In total, 2000 genes

Table 1
Top-10 lists of *Mus musculus* genes with largest ratios

Name	L-NNA	BSO	CloneID
(A) Top-10 L-NNA UP			
Ribosomal protein, large, P1 (Rplp1)	2.22	0.73	H3140H04
Postmeiotic segregation increased 2 (*S. cerevisiae*) (Pms2)	1.78	0.09	H3142E12
Ribosomal protein L8 (Rpl8)	1.58	1.09	H3141F09
Glycolipid transfer protein (LOC56356)	1.51	0.33	H3035F10
Sr104 protein	1.50	0.27	H3109F01
Cell-line C3H/RV polyubiquitin C (Ubc)	1.49	1.44	H3080D01
Gelsolin (Gsn)	1.34	0.97	H3120B07
Cytotoxic T-cell membrane glycoprotein Ly-3	1.31	0.69	H3119B11
Ribosomal protein, large, P1 (Rplp1)	1.22	0.76	H3124F09
Glyceraldehyde-3-phosphate dehydrogenase (Gapdh)	1.22	0.97	H3072A08
Syndecan 2 (Sdc2)	1.21	−0.15	H3148A01
(B) Top-10 BSO UP			
Putative homeodomain transcription factor (Phtf)	0.53	1.71	H3083F09
Ferritin L-subunit gene exons 1–4	0.85	1.58	H3023H09
Cell-line C3H/RV polyubiquitin C (Ubc)	1.49	1.44	H3080D01
E2F-like transcriptional repressor protein	0.58	1.44	H3126G09
Hepatoma-derived growth factor (Hdgf)	0.23	1.41	H3130E05
MAES-1	0.78	1.37	H3137H06
Ferritin light chain 1 (Ftl1)	0.94	1.35	H3011G06
Gamma-1 adducin (Addl)	0.57	1.27	H3122B01
Ribosomal protein, large, P1 (Rplp1)	1.01	1.26	H3124F08
Synapsin I (Syn1)	0.86	1.23	H3119A03
Ubiquitin C (Ubc)	0.37	1.19	H3124H09
(C) Top-10 L-NNA DOWN			
P53 binding protein 1	−2.11	−0.58	H3024H02
Brain calmodulin-dependent phosphatase (calcineurin) catalytic subunit	−1.52	0.20	H3110H11
CXCR-4	−1.51	−1.01	H3006D04
Transcriptional regulator protein (Hcngp-pending)	−1.48	−0.17	H3149G12
P8 protein (P8-pending)	−1.37	−0.99	H3106H03
Hyaluronidase 2 (Hyal2)	−1.34	0.10	H3145E12
Aryl-hydrocarbon receptor-interacting protein (Aip)	−1.31	−0.67	H3124C08
Programmed cell death 6 interacting protein (Pdcd6ip)	−1.30	−0.49	H3010F07
Hbs1-like (S. cerevisiae) (Hbs1l)	−1.25	−0.11	H3013B03
Ubiquitin-conjugating enzyme 7 (Ubce7)	−1.25	−0.36	H3011F10
(D) Top-10 BSO DOWN			
Seven in absentia 2 (Siah2)	−0.45	−2.38	H3092E12
Down syndrome critical region gene a (Dcra)	0.15	−2.16	H3007H01
Minopontin	−1.14	−1.50	H3082C12
Shank3b protein (Shank3)	0.05	−1.22	H3069C04
Niemann Pick type C1 (Npc1)	−1.06	−1.19	H3055G06
Plexin 3 (Plxn3)	0.23	−1.13	H3146C10
GLUT4 vesicle protein	−0.30	−1.08	H3094D04
P53-associated cellular protein PACT	−0.76	−1.07	H3090E12
Prolyl 4-hydroxylase alpha(I)-subunit	−1.15	−1.04	H3118E07
CXCR-4	−1.51	−1.01	H3006D04
Ornithine decarboxylase antizyme inhibitor (Oazi)	−0.16	−1.01	H3158B04

were annotated in 401 classes, with an average number of 8.3 genes per class. Thus, many genes were classified to more than one class. A selection based on the total number of genes per class (at least 10 genes) and at least 15% of genes significantly up or downregulated in at least one comparison is displayed in Fig. 4. For L-NNA, changes were most prominent in the category of genes involved in protein synthesis initiation and protein synthesis dephosphorylation and in embryogenesis and morphogenesis (all down). In the BSO-treated group, remarkable regulation of genes in energy metabolism was observed: glycolysis, fatty acid metabolism, tricarboxylic acid cycle, hydrogen transport, and ATP biosynthesis were all upregulated. For iron homeostasis, oxygen transport, and protein synthesis elongation, genes were prominently upregulated in both conditions.

Not all groups that contained interesting candidates were displayed in Fig. 4. These GO classes included transcription regulation, glutathione conjugation, and cell growth and maintenance (Supplementary Table 3). Several GO classes harbored some interesting genes, such as myocyte enhancer factor (Mef) 2α (0.82 for BSO and −0.11 for L-NNA) and chicken ovalbumin upstream promoter-transcription factor 2 (Coup-Tf2) (0.84 and −0.11, respectively) (transcription regulation), glutathione-*S* transferase mu (Gstm) 1 (1.04/1.07 and 1.02/0.44), Gstm2 (0.95 and 0.29), glutathione peroxidase (Gpx) 2 (0.18 and 0.92) and Gpx3 (0.78 and 0.56) (glutathione conjugation), pituitary tumor-transforming (Pttg) 1 (0.73 and 0.48), and necdin (Ndn) (0.74 and −0.87) (cell growth and maintenance), Cxcr4 (−1.0 and −1.5), stromal cell-derived factor (Sdf) 1β (−0.42 and −0.80) (chemotaxis), and several genes involved in ribosome biogenesis.

3.6. Detailed analysis of regulated genes of cell metabolism and protein synthesis genes in L-NNA- and BSO-treated mice

As a result of the remarkable regulation of so many genes involved in cell metabolism in BSO-treated mice, we looked one by one which genes were regulated by L-NNA and BSO. Genes in cell metabolism, regulated by either L-NNA or BSO, are shown in Fig. 5, superimposed on the pathway. A list of regulated genes involved in protein synthesis is displayed in Table 2, showing many protein synthesis genes are regulated in the same direction.

3.7. Transcription factor binding site analysis

Using Genomatix MatInspector, we searched for possible transcription factor binding sites in all differentially regulated glycolytic and respiratory chain genes. To avoid false positive results, a negative control set of 19 genes was also tested. The top-5 lists of results are shown in Table 3.

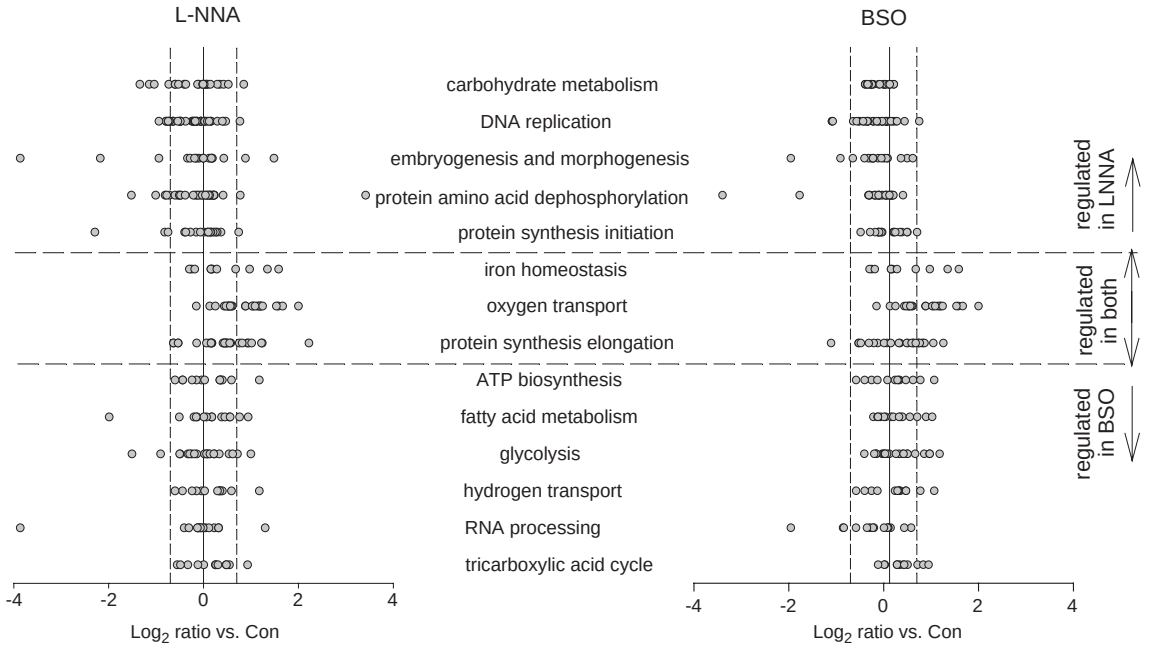

Fig. 4. Groups of biological processes (Gene Ontology) containing at least 10 genes and with at least 15% of genes significantly regulated in one condition are displayed. On the right side, the condition (Desikan et al., 2001) for which these groups are regulated is specified.

3.8. RT-PCR confirmed changed expression of glycolytic genes and glutathione metabolism

RT-PCR was performed on selected genes involved in different parts of cell metabolism. Gpi1 and Ech1 were both upregulated by L-NNA and BSO in the microarray experiment, which was confirmed by RT-PCR for BSO (Fig. 6). For L-NNA, a trend towards upregulation was observed. Atp5b and Gapdh, which were upregulated in both conditions on the chip, were now only upregulated with

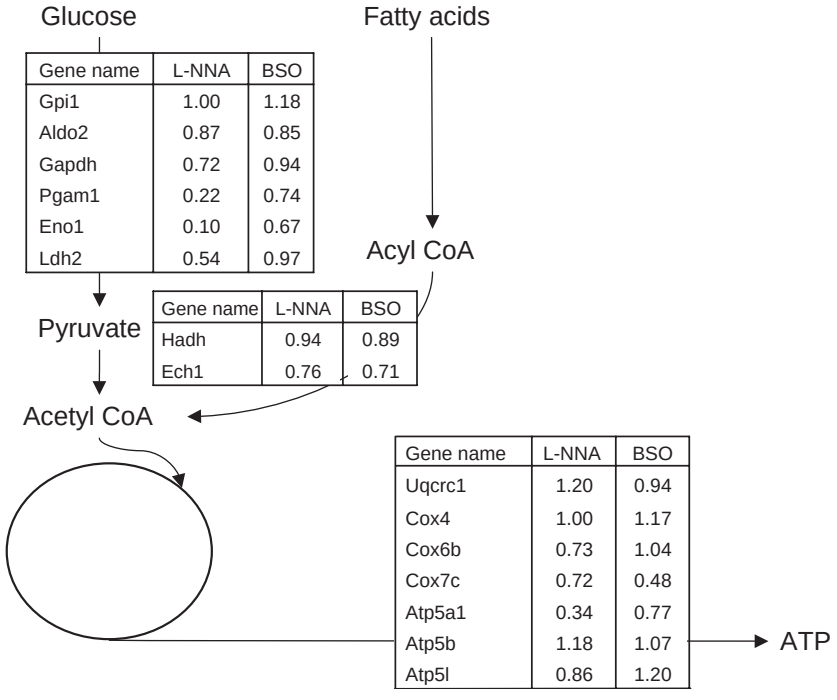

Gene name	L-NNA	BSO
Gpi1	1.00	1.18
Aldo2	0.87	0.85
Gapdh	0.72	0.94
Pgam1	0.22	0.74
Eno1	0.10	0.67
Ldh2	0.54	0.97

Gene name	L-NNA	BSO
Hadh	0.94	0.89
Ech1	0.76	0.71

Gene name	L-NNA	BSO
Uqcrc1	1.20	0.94
Cox4	1.00	1.17
Cox6b	0.73	1.04
Cox7c	0.72	0.48
Atp5a1	0.34	0.77
Atp5b	1.18	1.07
Atp5l	0.86	1.20

Fig. 5. Expression of cell metabolism genes in a diagram of metabolic pathway. Regulated genes are summarized in tables with their corresponding $\log_2$-transformed ratios for L-NNA and BSO superimposed on the pathway.

Table 2
Protein biosynthesis and protein synthesis elongation genes

Gene name	L-NNA	BSO	Clone ID
Ribosomal protein, large, P1 (Rplp1)	1.01	1.26	H3124F08
Ribosomal protein L8 (Rpl8)	1.58	1.09	H3141F09
Elongation factor 1-alpha (EF 1-alpha)	0.55	1.05	H3126H10
Ribosomal protein L10A (Rpl10a)	0.30	0.99	H3116A03
Ribosomal protein S12 (Rps12)	0.54	0.89	H3112B02
Ribosomal protein L12 (Rpl12)	0.14	0.88	H3113D05
Eukaryotic translation elongation factor 1-beta homolog (Eef1b)	0.75	0.86	H3118G07
Ribosomal protein L12 (Rpl12)	0.61	0.84	H3113D04
Ribosomal protein S7 (rpS7)	0.48	0.79	H3122C10
Ribosomal protein S15 (Rps15)	0.78	0.79	H3139D05
Ribosomal protein S8 (Rps8)	0.59	0.78	H3119A09
Ribosomal protein, large, P1 (Rplp1)	1.22	0.76	H3124F09
Ribosomal protein S6 (Rps6)	0.44	0.74	H3125H12
Protein synthesis elongation factor Tu (eEF-Tu, eEf-1-alpha)	0.43	0.74	H3133G05
Ribosomal protein, large, P1 (Rplp1)	2.22	0.73	H3140H04
Acidic ribosomal phosphoprotein PO (Arbp)	0.81	0.68	H3008E12
Protein synthesis elongation factor Tu (eEF-Tu, eEf-1-alpha)	0.95	0.62	H3126A06
Ribosomal protein L3 (Rpl3)	0.73	0.49	H3122F09
C-mos	0.88	0.40	H3084H01
Ribosomal protein S26 (Rps26)	0.92	0.25	H3120B03
Endothelial monocyte activating polypeptide 2 (Emap2)	0.72	0.22	H3155H05
MER9 processed pseudogene, elongation factor 2 related	0.83	0.10	H3033B09
Ribosomal protein S15 (Rps15)	0.93	0.05	H3150B01
Eukaryotic translation initiation factor 3 p42 subunit (Eif3p42)	0.73	−0.01	H3110H12
Ribosomal protein L3 (Rpl3)	−0.71	−0.54	H3011F03
Janus kinase 2 (Jak2)	−0.78	−0.36	H3049D07
Fibroblast growth factor inducible 13 (Fin13)	−0.81	−0.29	H3027F11
Protein phosphatase 5 (PP5)	−0.72	−0.15	H3158H01
Hbs1-like (S. cerevisiae) (Hbs1l)	−1.25	−0.11	H3013B03
Eukaryotic translation initiation factor 2B (Eif2b)	−0.82	−0.10	H3029H03
EIF-1A (eIF-1A)	−0.75	−0.09	H3008F08
E800	−1.08	0.06	H3004B09
Ufo	−0.73	0.19	H3152F05
Brain calmodulin-dependent phosphatase (calcineurin) catalytic subunit	−1.52	0.20	H3110H11
Focal adhesion kinase (Fadk)	−0.91	0.26	H3027G04
JAK1 protein tyrosine kinase	−0.64	1.00	H3059B07

BSO. Gstm1 and Gstm5 showed slight upregulation in the RT-PCR, in accordance with the microarray results.

4. Discussion

We report gene expression changes in the left ventricle of the heart in mice induced by mild pressure overload. NOS inhibition and glutathione depletion (i.e. decreased NO or increased $O_2^{\bullet-}$ availability) induced mild hypertension models without causing left ventricular hypertrophy. Both treatments decreased urinary NOx excretion, however, only BSO caused an increase in urinary thiobarbituric acid reactive substances and decreased liver total GSH. Microarray analysis of the left ventricles revealed differential gene expression in these two models. Among these were many co-regulated genes, such as ribosomal proteins, several glycolytic genes and components of the cytoskeleton and contractile apparatus, suggestive of adaptation to the higher afterload. Moreover, we identified genes that were specific to the model, such as glutathione peroxidase 2 for L-NNA, and Coup-Tf2 and Mef2α, Gstm1 and 2, and aldolase 1 for BSO. Further analysis of the biological function of the differentially expressed genes revealed an upregulation of metabolic genes with BSO, such as genes involved in glycolysis, fatty acid oxidation, and mitochondrial respiration, and upregulation of protein synthesis with L-NNA. Some of the expression changes in the glycolytic system were also observed in the L-NNA model, although less pronounced. The two models shared characteristics of early adaptation to pressure overload with regard to gene regulation of cell metabolism and contractility, although through different mechanisms of interference with the redox balance, as assessed from NOx and thiobarbituric acid reactive substances excretion and liver glutathione, and with different nuances regarding expression regulation.

Vaziri et al. (2000) have demonstrated that oxidative stress per se can induce arterial hypertension in rats. Similarly, NOS inhibition leads to severe hypertension in mice (Chatziantoniou et al., 1998). NO and $O_2^{\bullet-}$ are interrelated since NO can be scavenged by $O_2^{\bullet-}$ yielding peroxynitrite and NO can inhibit $O_2^{\bullet-}$ production via direct inhibition of NAD(P)H oxidase complex assembly (Clancy et al., 1992). In addition, the occurrence of myocardial infarction as a consequence of NO inhibition is dependent upon the presence of Ang II, which stimulates $O_2^{\bullet-}$ production by NAD(P)H oxidase in vascular cells (Verhagen et al., 2000). In the present study, NO and glutathione depletion caused a similar degree of hypertension, although both interventions interfere with different mechanisms regarding coronary blood flow, mitochondrial respiration/cardiac metabolism, and cardiac contractility. Both a decrease in NO (Kelm et al., 1997; Skjelbakken et al., 1996) and an increase in $O_2^{\bullet-}$ (Skjelbakken et al., 1996) diminish coronary blood flow, however, their potency to affect coronary perfusion is likely to be different. This may have consequences for coronary O_2 consumption and metabolism (Kelm et al., 1997). Furthermore, NO can inhibit mitochondrial respiration (Lizasoain et al., 1996). Thus, inhibition of NO could stimulate the respiratory chain. In contrast, $O_2^{\bullet-}$ inhibits the first step of the respiratory chain, NADH oxidoreductase, as was demonstrated in the superoxide dismutase $2^{+/-}$ mice (Van Remmen et al., 2001). Finally, NO itself can exert diverse influences on cardiac contractility. Since many studies do not take into account the differential localization of NOS isoforms, we refer to several studies with knockouts of different NOS isoforms. Neuronal NOS disruption leads to enhanced cardiac contractility

Table 3
Transcription factor binding sites in glycolytic and respiratory chain genes

TF-symbol	TF-Full name	Number of genes with TFBS	Number of TFBS in genes	Freq. in genes	Number of TFBS in NC	Freq. in NC	Difference
Glycolysis							
Oct1	Octamer-binding factor 1	6	7	1.17	11	0.58	0.59
Neurod1	Neurogenic differentiation 1	6	7	1.17	17	0.89	0.27
Comp1	Cooperates with myogenic proteins 1	5	8	1.33	18	0.95	0.39
Cdpcr3	Cut-like homeodomain protein 3	5	7	1.17	14	0.74	0.43
Pbx1	Pre-B-cell leukemia TF pseudogene 1	5	7	1.17	13	0.68	0.48
Nbre	NGFIB response element	5	5	0.83	8	0.42	0.41
Nrsf	Neural-restrictive silencer factor	5	5	0.83	9	0.47	0.36
Pax5	Paired box protein	5	5	0.83	13	0.68	0.15
Respiratory chain							
Comp1	Cooperates with myogenic proteins 1	7	10	1.67	18	0.95	0.72
Cdpcr3	CCAAT displacement protein 3	5	8	1.33	14	0.74	0.60
Hnf4	Hepatic nuclear factor 4	5	6	1.00	8	0.42	0.58
Yy1	Yin yang-1	5	6	1.00	8	0.42	0.58
Whn	Winged helix protein	5	11	1.83	15	0.79	1.04

A transcription factor (TF) binding site (TFBS) analysis was applied for regulated glycolytic and respiratory chain genes using Genomatix MatInspector. Those with the highest number of TFBS are displayed. The frequency of a TFBS is calculated as (Number of TFBS in genes or negative control)/(total number of genes in that group). The difference is calculated from the number of TFBS in the regulated genes and the negative control (NC) set.

(Barouch et al., 2002; Sears et al., 2003). Moreover, iNOS-deficient mice show improved contractile recovery after myocardial infarction (Sam et al., 2001). In contrast, mice lacking eNOS do not have changed contractile properties (Barouch et al., 2002). Therefore, a nonspecific NOS inhibitor, by affecting all NOS isoforms, potentially improves contractility, which indeed has been observed (Bartunek et al., 2000). In contrast, direct effects of reactive oxygen species on cardiac function can be summarized as impaired calcium handling by inhibiting Ca^{2+} efflux and enhancing influx leading to calcium overload and hence cellular injury. Thus, inhibition of NO and reactive oxygen species both lead to improved cardiac contractility. Hence, despite some overlap in their actions, quite different effects of NO inhibition and increased $O_2^{\bullet -}$ production on coronary blood flow, mitochondrial respiration and cardiac contractility can be anticipated, which likely has consequences for the transcriptional program, even though blood pressure responses were comparable.

Gene expression was in part similar between these two models. General features for pressure overload are changes in the contractile apparatus, cytoskeleton, and protein synthesis. Common expressional adaptations include increased expression of atrial natriuretic factor (Rockman et al., 1991; Tanaka et al., 1998), skeletal α-actin (Tanaka et al., 1998), β-tubulin (Collins et al., 1996; Mirotsou et al., 2003; Tagawa et al., 1996) and β-myosin heavy chain (Calderone et al., 1995; Zhang et al., 2003). Some of these were present on the chip. Despite the lack of left ventricular hypertrophy, we observed upregulation of tropomyosin isoform 2 and tubulin cofactor A, the latter being involved in the formation of tubulin polymers (Gao et al., 1993). Excess polymerization of tubulin is thought to hamper contractile function (Tsutsui et al., 1993) and increased tubulin protein expression was observed in humans (Zile et al., 2001) and in cats (Tsutsui et al., 1993) in response to pressure overload. Also, gelsolin, a calcium-dependent actin filament splitting protein that regulates cardiac L-type calcium channels (Lader et al., 1999) and is induced in human failing hearts (Yang et al., 2000), was upregulated in both models. Moreover, Mef2α, a TF regulating cardiac growth (Akazawa and Komuro, 2003) was upregulated in BSO but not L-NNA mice. Taken together, these models share common features of pressure overload as demonstrated by gene expression changes.

Cell expansion requires increased protein synthesis by enhancing translational efficiency (processing more transcripts simultaneously) and capacity (increasing the number of activated ribosomal components). Increased activation of elongation factors has been observed in pressure overload models (Nagatomo et al., 1999; Wada et al., 1996). In our study, even in the absence of left ventricular hypertrophy, protein synthesis apparently increased by upregulation of genes involved in initiation and elongation factors and ribosomal proteins in NOS inhibition, and, to a lesser extent, with glutathione depletion. However, increase in numbers of elongation factors is thought to be achieved by increased translation of pre-existing mRNA (Jefferies and Thomas, 1994) and not through mRNA induction of translational components. The upregulation was more pronounced in the NOS inhibition model, while there was no left ventricular hypertrophy, than with glutathione depletion, with a slight increase in heart weight. One could speculate that NO depletion and excess $O_2^{\bullet -}$ influence the machinery that is responsible for cardiac hypertrophy (Bartunek et al., 2000). These results may be indicative of early adaptations to pressure overload, before hypertrophy is apparent.

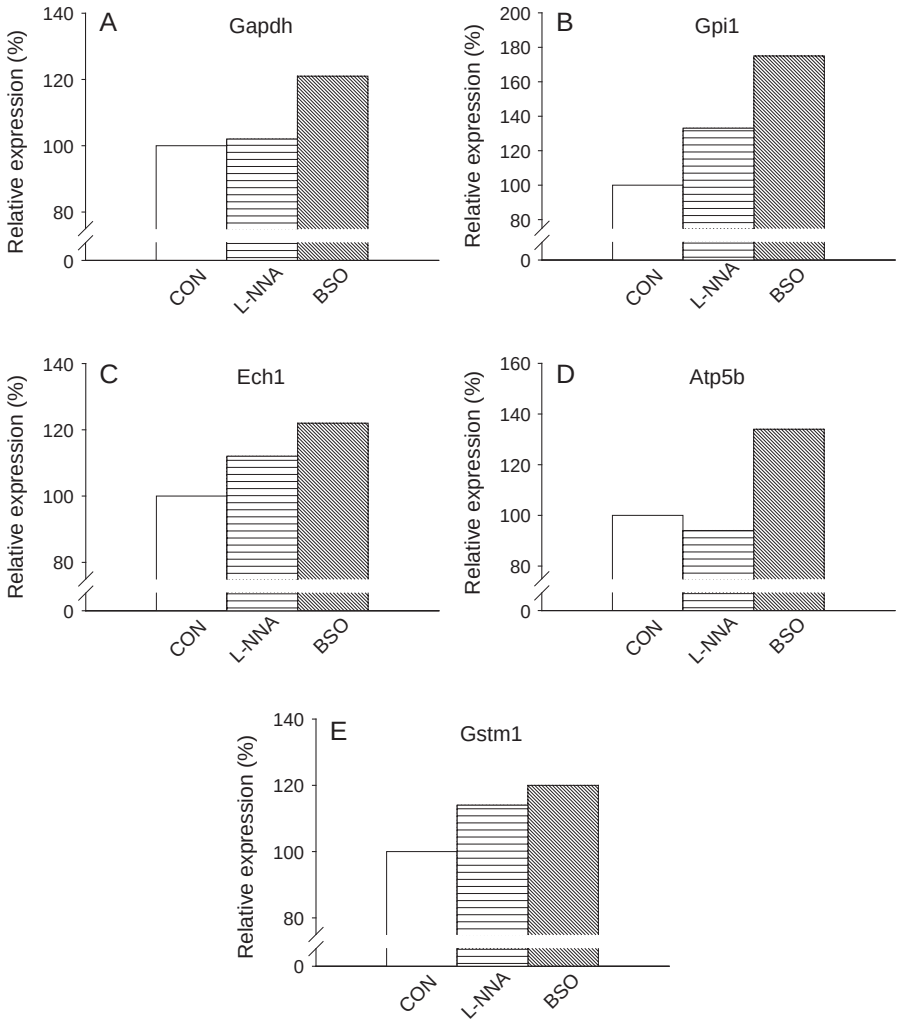

Fig. 6. RT-PCR confirmation of regulated genes on pooled samples. Expression values were corrected for 18S.

During increased cardiac workload, myocardial cells switch from fatty acid metabolism to glucose utilization to provide sufficient energy. Regulation of metabolic genes at the transcriptional level has been reported in hypertensive (Atlante et al., 1995), hypertrophied (Lydell et al., 2002) and failing hearts (Razeghi et al., 2001) as well as at the protein level in hypertensive hearts (Atlante et al., 1995). In our study, regulation of glycolytic genes was more pronounced in the BSO model, but was also present in the L-NNA mice. Interestingly, lactate dehydrogenase was only upregulated with BSO, suggesting that BSO mice rely on anaerobic glycolysis more than L-NNA mice, in line with the inhibiting effect of NO on mitochondrial respiration. At the same time, fatty acid oxidation and mitochondrial respiration genes were upregulated in both models. This might indicate a temporary compensation to maintain energy generation from fatty acids. Phosphofructokinase was not regulated at the transcriptional level in either L-NNA or BSO, possibly because this enzyme is regulated at the level of activity only. Nevertheless, the upregulation of the transcription factor Coup-Tf2, expressed during development but re-expressed in cardiac hypertrophy to regulate energy metabolism (Sack et al., 1997), could well indicate a coordinated regulation of the metabolic apparatus in BSO mice. The identification of possible targets of Coup-Tf2 in both the glycolytic pathway and mitochondrial respiration adds to this view. Summarizing, cardiac metabolism is regulated in both models, however, the enhancement of expression of glycolytic genes in glutathione-depleted hearts is more prominent.

Glutathione is an important determinant of the redox state of a tissue. In BSO-treated mice, liver GSH content was decreased, in line with previous reports (Vaziri et al., 2000). In the heart, GSH depletion could have large consequences as catalase is less abundant compared to glutathione peroxidase (Gpx), which is different from other tissues (Halliwell and Gutteridge, 1999). This may have resulted in the observed upregulation of Gpx3 in BSO-treated mice. Manganese superoxide dismutase, the predominant isoform in the heart, was not present on the array and catalase was not regulated. BSO upregulated Gstm1 and 2, which detoxify electrophilic compounds, including

products of oxidative stress, possibly as a compensatory defense mechanism. Interestingly, ferritin heavy and light chains were upregulated. This may indicate their role in preventing the formation of hydroxyl radicals in the Fenton reaction. We have demonstrated here again that manipulations with NO or $O_2^{\bullet-}$ result in very distinct regulation of gene expression of antioxidant pathways.

For both regulated glycolysis and respiratory chain genes, transcription factor binding sites for the transcription factor called cut-like homeodomain protein (Cdpcr) 3 were recognized frequently. Presumably, Cdpcr3 is regulated during development and differentiation, but not specifically in the heart (Nepveu, 2001). The transcription factor called COoperates with Myogenic Proteins (Comp) 1 interacts with myogenin, controlling myogenesis (Funk and Wright, 1992). For glycolytic genes, Pre-B-Cell leukemia transcription factor pseudogene (Pbx) 1 is involved in glucose tolerance (Kim and Kim, 2002; Naya et al., 1995). NGFIB response element (Nbre)-containing promoter sites, involved in cell proliferation (Labelle et al., 1999), were also found upstream of several glycolytic genes. For respiratory chain genes, sites for hepatic nuclear factor (Hnf) 4, a major regulator of glucose, cholesterol, and fatty acid metabolism, were highly present. The Yin Yang transcription factor is a regulator of acid alpha-glucosidase, important in glycogen storage in skeletal but not cardiac muscle (Yan et al., 2002). Thus, binding sites for a number of transcription factors were recognized of which some have been implicated in left ventricular hypertrophy and adaptation to pressure overload. The role of most of the mentioned transcription factors remains to be further elucidated.

The cause of essential hypertension is multifactorial and is frequently associated with left ventricular hypertrophy. In this study, we demonstrated that two different agents that interfere with blood pressure regulation result in partially overlapping gene expression responses in the heart. In this respect, it is remarkable that glutathione depletion and NO inhibition differentially affected genes in energy metabolism and protein synthesis. As such, expressional programs may affect the course of left ventricular hypertrophy development before overt hypertrophy is present depending upon the causative disturbance. Future studies should be directed to evaluate the translation of the gene expression responses to functional implications and to more severe models of hypertension with cardiac hypertrophy.

Acknowledgments

This study was financially supported by the Dutch Kidney Foundation (NSN6013). BB is a fellow of the Royal Dutch Academy of Arts and Sciences. We acknowledge the expert technical assistance of Paula Martens, Nel Willekes-Koolschijn, Henny IJzerman, Ria de Winter, Karin van 't Wout and Remmert de Roos.

Appendix A. Supplementary data

Supplementary data associated with this article can be found, in the online version, at doi:10.1016/j.ejphar.2005.01.054.

References

Akazawa, H., Komuro, I., 2003. Roles of cardiac transcription factors in cardiac hypertrophy. Circ. Res. 92, 1079–1088.

Ashburner, M., Ball, C.A., Blake, J.A., Botstein, D., Butler, H., Cherry, J.M., Davis, A.P., Dolinski, K., Dwight, S.S., Eppig, J.T., Harris, M.A., Hill, D.P., Issel-Tarver, L., Kasarskis, A., Lewis, S., Matese, J.C., Richardson, J.E., Ringwald, M., Rubin, G.M., Sherlock, G., 2000. Gene ontology: tool for the unification of biology. The Gene Ontology Consortium. Nat. Genet. 25, 25–29.

Atlante, A., Abruzzese, F., Seccia, T.M., Vulpis, V., Doonan, S., Pirrelli, A., Marra, E., 1995. Changes in enzyme levels in hypertensive heart tissue. Biochem. Mol. Biol. Int. 37, 983–990.

Attia, D.M., Ni, Z.N., Boer, P., Attia, M.A., Goldschmeding, R., Koomans, H.A., Vaziri, N.D., Joles, J.A., 2002. Proteinuria is preceded by decreased nitric oxide synthesis and prevented by a NO donor in cholesterol-fed rats. Kidney Int. 61, 1776–1787.

Attia, D.M., Goldschmeding, R., Attia, M.A., Boer, P., Koomans, H.A., Joles, J.A., 2003. Male gender increases sensitivity to renal injury in response to cholesterol loading. Am. J. Physiol., Renal Physiol. 284, F718–F726.

Barouch, L.A., Harrison, R.W., Skaf, M.W., Rosas, G.O., Cappola, T.P., Kobeissi, Z.A., Hobai, I.A., Lemmon, C.A., Burnett, A.L., O'Rourke, B., Rodriguez, E.R., Huang, P.L., Lima, J.A., Berkowitz, D.E., Hare, J.M., 2002. Nitric oxide regulates the heart by spatial confinement of nitric oxide synthase isoforms. Nature 416, 337–339.

Bartunek, J., Weinberg, E.O., Tajima, M., Rohrbach, S., Katz, S.E., Douglas, P.S., Lorell, B.H., 2000. Chronic *N*(G)-nitro-L-arginine methyl ester-induced hypertension : novel molecular adaptation to systolic load in absence of hypertrophy. Circulation 101, 423–429.

Bradford, M.M., 1976. A rapid and sensitive method for the quantitation of microgram quantities of protein utilizing the principle of protein-dye binding. Anal. Biochem. 72, 248–254.

Calderone, A., Takahashi, N., Izzo Jr., N.J., Thaik, C.M., Colucci, W.S., 1995. Pressure- and volume-induced left ventricular hypertrophies are associated with distinct myocyte phenotypes and differential induction of peptide growth factor mRNAs. Circulation 92, 2385–2390.

Chatziantoniou, C., Boffa, J.J., Ardaillou, R., Dussaule, J.C., 1998. Nitric oxide inhibition induces early activation of type I collagen gene in renal resistance vessels and glomeruli in transgenic mice. Role of endothelin. J. Clin. Invest. 101, 2780–2789.

Chon, H., Gaillard, C.A., van der Meijden, B.B., Dijstelbloem, H.M., Kraaijenhagen, R.J., van Leenen, D., Holstege, F.C., Joles, J.A., Bluyssen, H.A., Koomans, H.A., Braam, B., 2004. Broadly altered gene expression in blood leukocytes in essential hypertension is absent during treatment. Hypertension 43, 947–951.

Clancy, R.M., Leszczynska-Piziak, J., Abramson, S.B., 1992. Nitric oxide, an endothelial cell relaxation factor, inhibits neutrophil superoxide anion production via a direct action on the NADPH oxidase. J. Clin. Invest. 90, 1116–1121.

Collins, J.F., Pawloski-Dahm, C., Davis, M.G., Ball, N., Dorn II, G.W., Walsh, R.A., 1996. The role of the cytoskeleton in left ventricular pressure overload hypertrophy and failure. J. Mol. Cell. Cardiol. 28, 1435–1443.

Depre, C., Shipley, G.L., Chen, W., Han, Q., Doenst, T., Moore, M.L., Stepkowski, S., Davies, P.J., Taegtmeyer, H., 1998. Unloaded heart in

vivo replicates fetal gene expression of cardiac hypertrophy. Nat. Med. 4, 1269–1275.

Desikan, R., S, A.H.-M., Hancock, J.T., Neill, S.J., 2001. Regulation of the Arabidopsis transcriptome by oxidative stress. Plant Physiol. 127, 159–172.

Funk, W.D., Wright, W.E., 1992. Cyclic amplification and selection of targets for multicomponent complexes: myogenin interacts with factors recognizing binding sites for basic helix-loop-helix, nuclear factor 1, myocyte-specific enhancer-binding factor 2, and COMP1 factor. Proc. Natl. Acad. Sci. U. S. A. 89, 9484–9488.

Gao, Y., Vainberg, I.E., Chow, R.L., Cowan, N.J., 1993. Two cofactors and cytoplasmic chaperonin are required for the folding of alpha- and beta-tubulin. Mol. Cell. Biol. 13, 2478–2485.

Halliwell, B., Gutteridge, J.M., 1999. Antioxidant Defences Free Radicals in Biology and Medicine. Oxford, Oxford, U.P., pp. 105–245.

Hoenderop, J.G., Chon, H., Gkika, D., Bluyssen, H.A., Holstege, F.C., St-Arnaud, R., Braam, B., Bindels, R.J., 2004. Regulation of gene expression by dietary Ca2+ in kidneys of 25-hydroxyvitamin D3-1 alpha-hydroxylase knockout mice. Kidney Int. 65, 531–539.

Jefferies, H.B., Thomas, G., 1994. Elongation factor-1 alpha mRNA is selectively translated following mitogenic stimulation. J. Biol. Chem. 269, 4367–4372.

Kelm, M., Schafer, S., Dahmann, R., Dolu, B., Perings, S., Decking, U.K., Schrader, J., Strauer, B.E., 1997. Nitric oxide induced contractile dysfunction is related to a reduction in myocardial energy generation. Cardiovasc. Res. 36, 185–194.

Kim, H.J., Kim, S.G., 2002. Alterations in cellular Ca(2+) and free iron pool by sulfur amino acid deprivation: the role of ferritin light chain down-regulation in prooxidant production. Biochem. Pharmacol. 63, 647–657.

Labelle, Y., Bussieres, J., Courjal, F., Goldring, M.B., 1999. The EWS/TEC fusion protein encoded by the t(9;22) chromosomal translocation in human chondrosarcomas is a highly potent transcriptional activator. Oncogene 18, 3303–3308.

Lader, A.S., Kwiatkowski, D.J., Cantiello, H.F., 1999. Role of gelsolin in the actin filament regulation of cardiac L-type calcium channels. Am. J. Physiol. 277, C1277–C1283.

Lim, D.S., Roberts, R., Marian, A.J., 2001. Expression profiling of cardiac genes in human hypertrophic cardiomyopathy: insight into the pathogenesis of phenotypes. J. Am. Coll. Cardiol. 38, 1175–1180.

Lizasoain, I., Moro, M.A., Knowles, R.G., Darley-Usmar, V., Moncada, S., 1996. Nitric oxide and peroxynitrite exert distinct effects on mitochondrial respiration which are differentially blocked by glutathione or glucose. Biochem. J. 314 (Pt. 3), 877–880.

Lydell, C.P., Chan, A., Wambolt, R.B., Sambandam, N., Parsons, H., Bondy, G.P., Rodrigues, B., Popov, K.M., Harris, R.A., Brownsey, R.W., Allard, M.F., 2002. Pyruvate dehydrogenase and the regulation of glucose oxidation in hypertrophied rat hearts. Cardiovasc. Res. 53, 841–851.

Matsubara, B.B., Matsubara, L.S., Zornoff, L.A., Franco, M., Janicki, J.S., 1998. Left ventricular adaptation to chronic pressure overload induced by inhibition of nitric oxide synthase in rats. Basic Res. Cardiol. 93, 173–181.

Mirotsou, M., Watanabe, C.M., Schultz, P.G., Pratt, R.E., Dzau, V.J., 2003. Elucidating the molecular mechanism of cardiac remodeling using a comparative genomic approach. Physiol. Genomics 15, 115–126.

Nagatomo, Y., Carabello, B.A., Hamawaki, M., Nemoto, S., Matsuo, T., McDermott, P.J., 1999. Translational mechanisms accelerate the rate of protein synthesis during canine pressure-overload hypertrophy. Am. J. Physiol. 277, H2176–H2184.

Naya, F.J., Stellrecht, C.M., Tsai, M.J., 1995. Tissue-specific regulation of the insulin gene by a novel basic helix-loop-helix transcription factor. Genes Dev. 9, 1009–1019.

Nepveu, A., 2001. Role of the multifunctional CDP/Cut/Cux homeodomain transcription factor in regulating differentiation, cell growth and development. Gene 270, 1–15.

Razeghi, P., Young, M.E., Alcorn, J.L., Moravec, C.S., Frazier, O.H., Taegtmeyer, H., 2001. Metabolic gene expression in fetal and failing human heart. Circulation 104, 2923–2931.

Rockman, H.A., Ross, R.S., Harris, A.N., Knowlton, K.U., Steinhelper, M.E., Field, L.J., Ross Jr., J., Chien, K.R., 1991. Segregation of atrial-specific and inducible expression of an atrial natriuretic factor transgene in an in vivo murine model of cardiac hypertrophy. Proc. Natl. Acad. Sci. U. S. A. 88, 8277–8281.

Sack, M.N., Disch, D.L., Rockman, H.A., Kelly, D.P., 1997. A role for Sp and nuclear receptor transcription factors in a cardiac hypertrophic growth program. Proc. Natl. Acad. Sci. U. S. A. 94, 6438–6443.

Sam, F., Sawyer, D.B., Xie, Z., Chang, D.L., Ngoy, S., Brenner, D.A., Siwik, D.A., Singh, K., Apstein, C.S., Colucci, W.S., 2001. Mice lacking inducible nitric oxide synthase have improved left ventricular contractile function and reduced apoptotic cell death late after myocardial infarction. Circ. Res. 89, 351–356.

Sambandam, N., Lopaschuk, G.D., Brownsey, R.W., Allard, M.F., 2002. Energy metabolism in the hypertrophied heart. Heart Fail. Rev. 7, 161–173.

Sears, C.E., Bryant, S.M., Ashley, E.A., Lygate, C.A., Rakovic, S., Wallis, H.L., Neubauer, S., Terrar, D.A., Casadei, B., 2003. Cardiac neuronal nitric oxide synthase isoform regulates myocardial contraction and calcium handling. Circ. Res. 92, e52–e59.

Skjelbakken, T., Valen, G., Vaage, J., 1996. Perfusing isolated rat hearts with hydrogen peroxide: an experimental model of cardiac dysfunction caused by reactive oxygen species. Scand. J. Clin. Lab. Invest. 56, 431–439.

Tagawa, H., Rozich, J.D., Tsutsui, H., Narishige, T., Kuppuswamy, D., Sato, H., McDermott, P.J., Koide, M., Cooper, G.t., 1996. Basis for increased microtubules in pressure-hypertrophied cardiocytes. Circulation 93, 1230–1243.

Tanaka, N., Ryoke, T., Hongo, M., Mao, L., Rockman, H.A., Clark, R.G., Ross Jr., J., 1998. Effects of growth hormone and IGF-I on cardiac hypertrophy and gene expression in mice. Am. J. Physiol. 275, H393–H399.

Tsutsui, H., Ishihara, K., Cooper, G.t., 1993. Cytoskeletal role in the contractile dysfunction of hypertrophied myocardium. Science 260, 682–687.

Van Remmen, H., Williams, M.D., Guo, Z., Estlack, L., Yang, H., Carlson, E.J., Epstein, C.J., Huang, T.T., Richardson, A., 2001. Knockout mice heterozygous for Sod2 show alterations in cardiac mitochondrial function and apoptosis. Am. J. Physiol., Heart Circ. Physiol. 281, H1422–H1432.

Vaziri, N.D., Wang, X.Q., Oveisi, F., Rad, B., 2000. Induction of oxidative stress by glutathione depletion causes severe hypertension in normal rats. Hypertension 36, 142–146.

Verhagen, A.M., Hohbach, J., Joles, J.A., Braam, B., Boer, P., Koomans, H.A., Grone, H., 2000. Unchanged cardiac angiotensin II levels accompany losartan-sensitive cardiac injury due to nitric oxide synthase inhibition. Eur. J. Pharmacol. 400, 239–247.

Wada, H., Ivester, C.T., Carabello, B.A., Cooper, G.t., McDermott, P.J., 1996. Translational initiation factor eIF-4E. A link between cardiac load and protein synthesis. J. Biol. Chem. 271, 8359–8364.

Werner, T., 2001. Target gene identification from expression array data by promoter analysis. Biomol. Eng. 17, 87–94.

Yan, B., Raben, N., Plotz, P.H., 2002. Hes-1, a known transcriptional repressor, acts as a transcriptional activator for the human acid alpha-glucosidase gene in human fibroblast cells. Biochem. Biophys. Res. Commun. 291, 582–587.

Yang, J., Moravec, C.S., Sussman, M.A., DiPaola, N.R., Fu, D., Hawthorn, L., Mitchell, C.A., Young, J.B., Francis, G.S., McCarthy, P.M., Bond, M., 2000. Decreased SLIM1 expression and increased gelsolin expression in failing human hearts measured by high-density oligonucleotide arrays. Circulation 102, 3046–3052.

You, S.A., Archacki, S.R., Angheloiu, G., Moravec, C.S., Rao, S., Kinter, M., Topol, E.J., Wang, Q., 2003. Proteomic approach to coronary atherosclerosis shows ferritin light chain as a significant marker:

evidence consistent with iron hypothesis in atherosclerosis. Physiol. Genomics 13, 25–30.

Zhang, Y., Carreras, D., de Bold, A.J., 2003. Discoordinate re-expression of cardiac fetal genes in N(omega)-nitro-L-arginine methyl ester (L-NAME) hypertension. Cardiovasc. Res. 57, 158–167.

Zile, M.R., Green, G.R., Schuyler, G.T., Aurigemma, G.P., Miller, D.C., Cooper, G.t., 2001. Cardiocyte cytoskeleton in patients with left ventricular pressure overload hypertrophy. J. Am. Coll. Cardiol. 37, 1080–1084.